Progress In Electromagnetics Research C, Vol. 97, 213–225, 2019

Wide Axial Ratio Bandwidth, High Gain, and Low Profile Cavity Backed Circularly Polarized Elliptical Array for Satellite Applications

Alla M. Eid, Amgad A. Salama*, and Hassan M. Elkamchouchi

Abstract—In this paper, a novel wide axial ratio bandwidth (ARBW), high gain, and low profile left-hand circularly polarized [4 × 4] elliptical microstrip array suitable for Ku-band satellite TV reception applications is introduced. A careful study has been done to get the optimum design to be suited for these application requirements. A circularly polarized microstrip patch with two stubs opposite to each other to produce two orthogonal modes is presented. The proposed element has 1.49 GHz 10-dB return loss bandwidth (RLBW), 0.44 GHz 3-dB Axial-ratio band (ARBW), and 6.9 dBi gain. A novel substrate integrated waveguide (SIW) feeding structure is investigated. Using the advantage of the output ports phase response of the SIW feeding network, two structures have been investigated. First, a [2 × 2] circular array has been designed, and although it has reached a good RLBW, this structure does not achieve the required ARBW for the above-mentioned application. Further, a compact [2 × 2] sequential feeding network is designed to widen the ARBW. The measurement shows a very good result with about 12 dBi gain, 14.8% RLBW, and 12% ARBW. Finally, a [4 × 4] duple sequential feeding array is designed to increase the gain of the antenna to about 19 dBi, with 13% RLBW and 20.7% ARBW. In addition to that, the final antenna profile is 0.0184λ.

1. INTRODUCTION

Almost all of the satellite applications such as satellite TV broadcasting, satellite phone, navigation, geo-imaging, weather forecasting, and data distribution prefer circularly polarized antennas for many reasons [1]. Firstly, it is effective against multi-path interference and fading because circularly polarized (CP) antennas have a high co-polarized to x-polarized ratio difference. Secondly, it reduces losses due to Faraday rotation in the ionosphere to about 3-dB more than the linear polarized one. Finally, there is no mismatch between the transmitter and receiver due to no restriction in the rotation of the transmitter antenna to the receiver.

For Ku band satellite TV reception application [2, 3] wide return loss (RL), axial ratio (AR) bandwidths, and high gain, along with small size and low profile are required. A lot of researches have been done to achieve these requirements [2–9], where in [4], a [2 × 2] circularly polarized microstrip array has been used along with a substrate integrated waveguide (SIW) to back feed each element, and the design is in low cost with a low profile. However, it suffers from narrow RLBW as well as ARBW. In [5], Li et al., introduced a 60 GHz SIW circularly polarized antenna with 10.7% ARBW. Yet, the design is complex as they used low temperature cofired ceramic (LTCC) technology and had a large profile ($.39\lambda_o$) (λ_o refers to the wavelength of the lowest operating frequency). In [7], the LTCC technology was utilized for a 60 GHz circularly polarized antenna array. Using [4 × 4] helical elements, wide RL and AR bandwidths were achieved; however, the design had a large profile ($.4\lambda_o$) and high

Received 1 October 2019, Accepted 23 November 2019, Scheduled 13 December 2019
* Corresponding author: Amgad A. Salama (amgad.salama@ieee.org).
The authors are with Electrical Engineering Department, Faculty of Engineering, Alexandria University, Alexandria, Egypt.

complexity. On the other hand, a very low profile ($.05\lambda_o$) was achieved using a [16×6] array in [2]. Unfortunately, both of the RLBW and ARBW are about 6.16% and 8.2%, respectively. In [3], using a [16×1] spiral antenna array, the required ARBW and RLBW were achieved, but it needs a complex feeding network.

In our work, we divide the antenna design to three main parts that control the antenna response, the radiator element, feeding network, and antenna array structure (linear, planner, circular, elliptical). Table 1 illustrates different types of antenna elements along with their RLBW, ARBW, as well as their pros and cons. While Table 2 states the main difference between the feeding network types. For the array structure, we take the study in [10] that made a comparison between uniform rectangular array (URA), uniform circular array (UCA), and planner circular array (PCA) with the same number of elements with three different algorithms, which got a conclusion that the UCA achieved the highest directivity in the three algorithms.

From Tables 1 and 2, we choose a microstrip patch antenna as a radiator because of its advantages in size and profile. SIW has been used for the feeding network because of its advantages in size, power capability, appropriate BW, and profile to construct a cavity with slot to back feed the array, where the cavity back feeding reduces the mutual coupling between the elements and improve the overall gain and efficiency [4]. Using microstrip patch makes limitation in ARBW, so we decide to use the sequential

Table 1. Different element types comparison.

Ref.	Type	RLBW (%)	ARBW (%)	Advantage	Disadvantage
[1, 11–13]	Patch antenna (single feed)	(2.1 : 5)	(0.8 : 5)	low size low profile easy fabrication easy to integrate low coast medium efficency	low RLBW low ARBW
[1, 14, 15]	Patch antenna (multiple feed)	(32 : 54.75)	(8.7 : 42.6)	medium RLBW medium RLBW low profile low cost easy to fabricate medium efficency	large size
[1, 16–18]	Wired antenna (Helix, QHA)	(0.8 : 10)	(0.5 : 12)	large RLBW large ARBW low coast easy to fabricate	large size large profile low efficency
[1, 19–22]	Dielectric antenna	(5.4 : 33)	(1.95 : 10)	large RLBW medium ARBW medium size low coast easy to fabricate high efficency	large profile
[1, 23–26]	Microstrip Slotted antenna	(12.4 : 39)	(4.3 : 12)	large RLBW medium ARBW low coast low profile easy to fabricate	large size low gain

Table 2. Feeding networks comparison.

Ref.	Type	Advantage	Disadvantage
[1]	Microstrip line	low size low profile easy to fabracate easy to integtrate low coast	low bandwidth low efficency not sufficient for high power low efficiency poor isolation among adjacent lines
[27]	Strip line	has a greater frequency bandwidth lower radiation loss better isolation EM shielding can be achieved	complex and expensive in fabricating large profile tuning or troubleshooting is complex
[28]	Waveguide	high power handling capacity has lower attenuation its simple structure on both the ends EM fields are shielded from outside	very bulky in size and weight not economical narrow band of operation TEM mode of propagation is not possible not suitable for operations at lower frequencies
[29, 30]	SIW	cost effective easy to fabricate no bulky transitions between elements Provide inherent shielding from the outer	leakage losses dielectric losses exhibits cutoff frequency of lower values

feeding technique to improve the ARBW and exploit the phase behavior of the cavity to enhance the design compactability.

This paper is organized as follows. Following this introduction, the paper is divided into six sections. In Section 2, a circularly polarized element is introduced. A $[2 \times 2]$ initial circular array coupled by slotted cavity back SIW design and its power divider are proposed in Section 3. In Section 4, a $[2 \times 2]$ elliptical sequential fed array coupled by slotted cavity back SIW design and its feeding power divider are presented. A $[4 \times 4]$ elliptical array is introduced in Section 5. Finally, Section 6 illustrates the results followed by the conclusion in Section 7.

2. CIRCULAR POLARIZED ELEMENT

The main concept to produce a circularly polarized pattern is to generate two equal and orthogonal electric field components, E, at the far field. The electric field of the antenna can be illustrated as given in Eq. (1). In order to produce the circular polarization, the condition in Eqs. (2) and (3) must be achieved [1]. Consequently a new microstrip circular patch antenna with two opposite stubs is designed as shown in Fig. 1.

$$E(\theta, \phi) = \theta E_\theta(\theta, \phi) e^{j\phi_1} + \phi E_\phi(\theta, \phi) e^{j\phi_2} \tag{1}$$

$$E_\theta(\theta, \phi) = E_\phi(\theta, \phi) \tag{2}$$

$$\phi_1 - \phi_2 = \pm \frac{pi}{2} \tag{3}$$

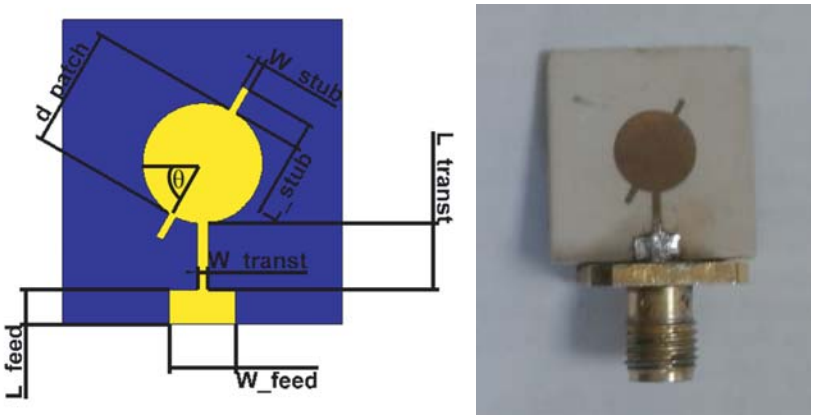

(a) (b)

Figure 1. Configuration of (a) the circular polarized element and (b) the fabricated one.

where E_θ (θ, ϕ), E_ϕ (θ, ϕ) are the magnitudes of electric field components, and ϕ_1 and ϕ_2 denote the phase shifts of field components.

[31] illustrates that both of the substrate thickness and the dielectric constant control the quality factor (Q) as given in Eq. (4). From Eqs. (5) and (6), it can be seen that quality factor (Q) is inversely proportional to the RLBW and ARBW.

$$\frac{1}{Q_t} = \frac{1}{Q_{rad}} + \frac{1}{Q_c} + \frac{1}{Q_d} + \frac{1}{Q_{sw}} \tag{4}$$

$$\text{ARBW} = \frac{\text{AR} - 1}{Q\sqrt{\text{AR}}} \tag{5}$$

$$\text{RLBW} = \frac{\sqrt{2\,(\text{VSWR} - 1)}}{Q} \tag{6}$$

where Q_t = total quality factor, Q_{rad} = quality factor due to radiation(space wave) losses, Q_c = quality factor due to conduction (ohmic) losses, Q_d = quality factor due to dielectric losses, Q_{sw} = quality factor due to surface waves.

So, by lowering the quality factor, wider bandwidth is obtained, and consequently, using material with low ϵ_r and high thickness (h) is recommended [1]. The patch is designed using Rogers 3003 with dielectric constant $\epsilon_r = 3$, substrate height $h = 1.524$ mm, and loss tangent $\delta = 0.0013$. The patch antenna is designed according to Eqs. (7) and (8) [1] where final parameters of the antenna are given in Table 3.

$$\text{R}_{\text{patch}} = \frac{F}{\sqrt{1 + \frac{200h}{\pi\epsilon_r F}\{\ln(\frac{BF}{200h}) + 1.7726\}}} \tag{7}$$

$$F = \frac{8.791 \times 10^9}{f_o\sqrt{\epsilon_r}} \tag{8}$$

Figure 2 illustrates the simulation and measurement results of the proposed circular patch. It can be seen that changing the rotation angle, θ, affects both of RL and AR bandwidths in addition to the type of polarization. For $\theta = 60°$ and 110°, the RLBWs, ARBWs, and realized gains are almost the same as can be seen from Figures 2(a), (b), and (c), respectively. However, from Figures 2(d) and (e), the polarization types are different. It is clear from Figures 2(f) and (g) that two orthogonal clockwise rotating modes will be generated, and consequentially, an LHCP field is propagated following the right-hand rule. The result illustrated in Figure 2(h) shows that the operating simulation and measurement 10-dB bandwidths are between 11.3 and 12.37 GHz (8.9% BW), and between 10.89 and 12.33 GHz (12% BW), respectively. A 3-dB simulated ARBW is from 12.01 to 12.36 GHz (3% BW), while the measured

Table 3. Final optimized element parameter values.

parameter	description	Value
D_{patch}	Patch diameter	13.8 mm
L_{stub}	Stub length	1.7 mm
W_{stub}	Stub width	0.45 mm
θ	Rotation angle	60°
L_{feed}	Feeding length	2.00 mm
W_{feed}	Feeding width	3.8 mm
L_{transt}	Transition length	3.18 mm
W_{transt}	Transition width	0.2 mm
L_{sub}	Substrate length	17.47 mm
W_{sub}	Substrate width	16.04 mm

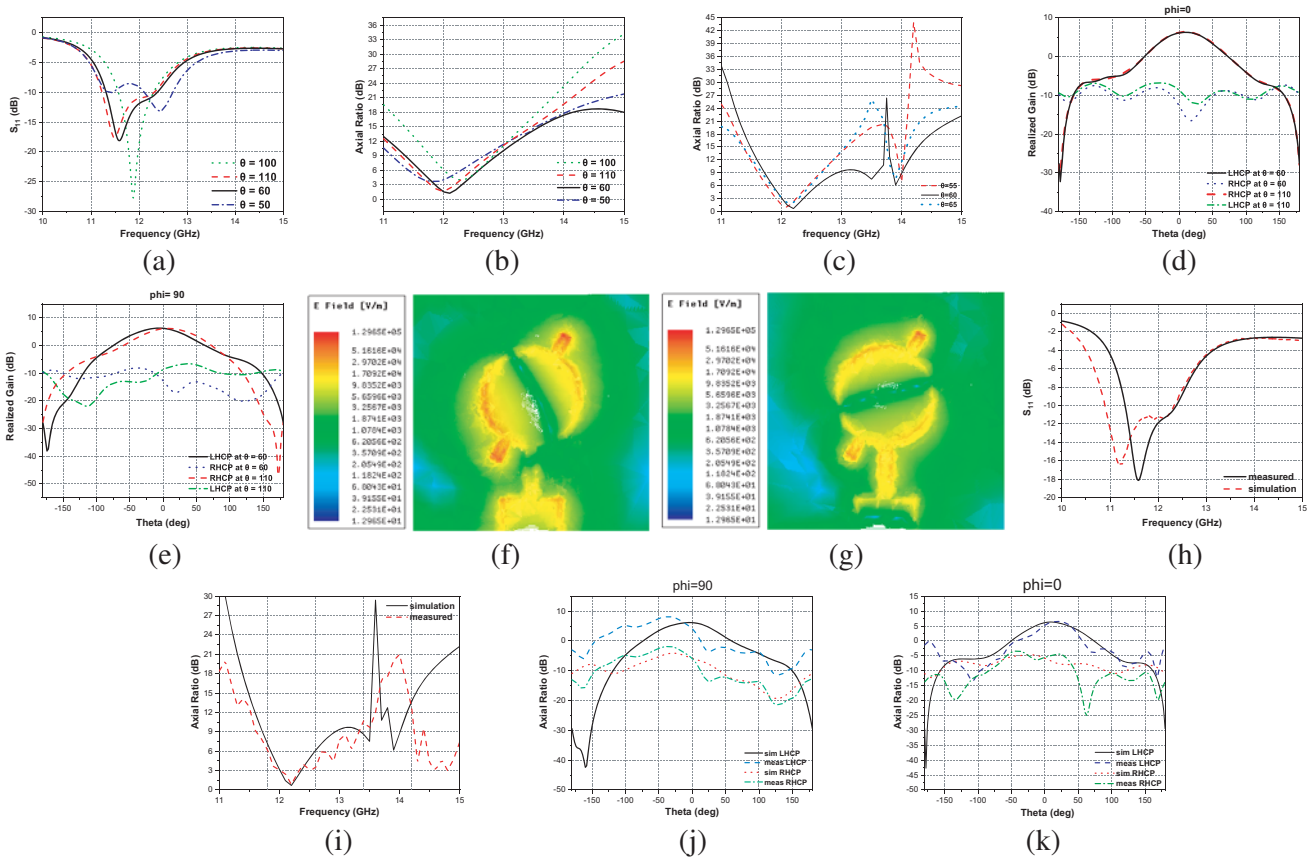

Figure 2. Simulation and measurement results of the circular patch, where (a), (b), and (c) are the simulation RL, AR, and the realized gain at various values of θ in dB. (d) and (e) are comparison between the realized gain at $\theta = 60$ and 110 at $\phi = 0°$ and 90°, respectively. (f) and (g) The electric fields at $\frac{1}{4}$ and $\frac{3}{4}$ of a period time (T), respectively, at 12.3 GHz. (h) Comparison between simulated and measured RLs. (i) Comparison between simulated and measured ARs. (j) and (k) Comparison between simulated and measured LHCPs and RHCPs at $\phi = 90°$ and 0°, respectively.

result is from 12.01 to 12.33 GHz (2.7% BW) as shown in Figure 2(i). A good agreement between simulation and measurement results shows that the antenna gain is about 6.5 dBi at 12.3 GHz and the LHCP to RHCP ratio more than 11 dBi on the broadside direction.

3. [2 × 2] INITIAL CIRCULAR ARRAY COUPLED BY SLOTTED CAVITY BACK SIW DESIGN

In order to overcome the free space loss between the transmitter and receiver, a high gain is recommended in the antenna specification. Therefore, the initial [2 × 2] circular array is designed as shown in Fig. 4(a). The proposed initial array consists of two main parts. The first part is a 4-way equal power divider fed by a slot at the top of SIW with four short vias with distance L_{cavity} to construct a cavity resonator with opening $W_{openning}$ as shown in Figs. 3(a) and (b), while the second part is the radiator element. The power divider's results show that port 3 and port 4 are with equal amplitude, however, 180° out of phase to ports 2 and 5, as given in Figs. 3(c) and (d). The power divider's phase response facilitates the generation of two orthogonal modes without any extra transmission lines as illustrated in Figs. 4(d) and (e) by adjusting the element rotation. The optimized design parameters are illustrated in Table 4.

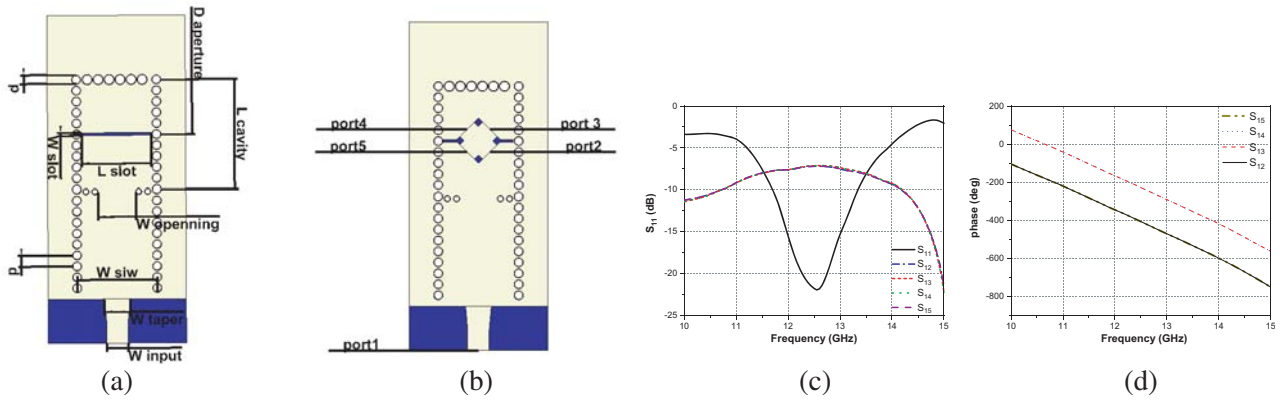

Figure 3. A 4-way power divider with SIW slotted cavity. (a) Front view of the structure, (b) the divider ports, (c) RL and the outputs insertion loss in dB, and (d) the phase response of the output ports.

Simulation RL, AR, and the realized gain of the initial array design are presented in Figs. 4(b), (c), and (d), respectively. Changing the cavity length (L_{cavity}) has a great effect on the RL, as shown in Fig. 4(a); however, it does not affect the AR. Choosing the cavity length, L_{cavity} = 22 mm, gives a better RLBW from 11.7 to 13.14 GHz (12% BW) and good gain about 10 dB, but a poor ARBW between 11.54 and 11.94 GHz (3.3% BW) and low co-polarized to x-polarized ratio only 8 dB in the broadside direction. Figs. 4(e) and (f) show that the LHCP will be produced due to the electric field rotation in clockwise as the right-hand rule.

4. [2 × 2] ELLIPTICAL ARRAY SEQUENTIAL FEEDING

In order to overcome the narrow band AR of the [2 × 2] array, a sequential feeding technique is used, which is proven to be an effective method to increase the ARBW [2, 32]. Taking the advantage of the previously illustrated feeding network along with adding two more quarter-wave transmission lines at ports 3 and 5, as presented in Fig. 5(a), four orthogonal outputs are generated, as shown in Fig. 5(b). Consequently, an elliptical array with optimized stub length and element position is illustrated in Fig. 6. The optimized design parameters are shown in Table 5.

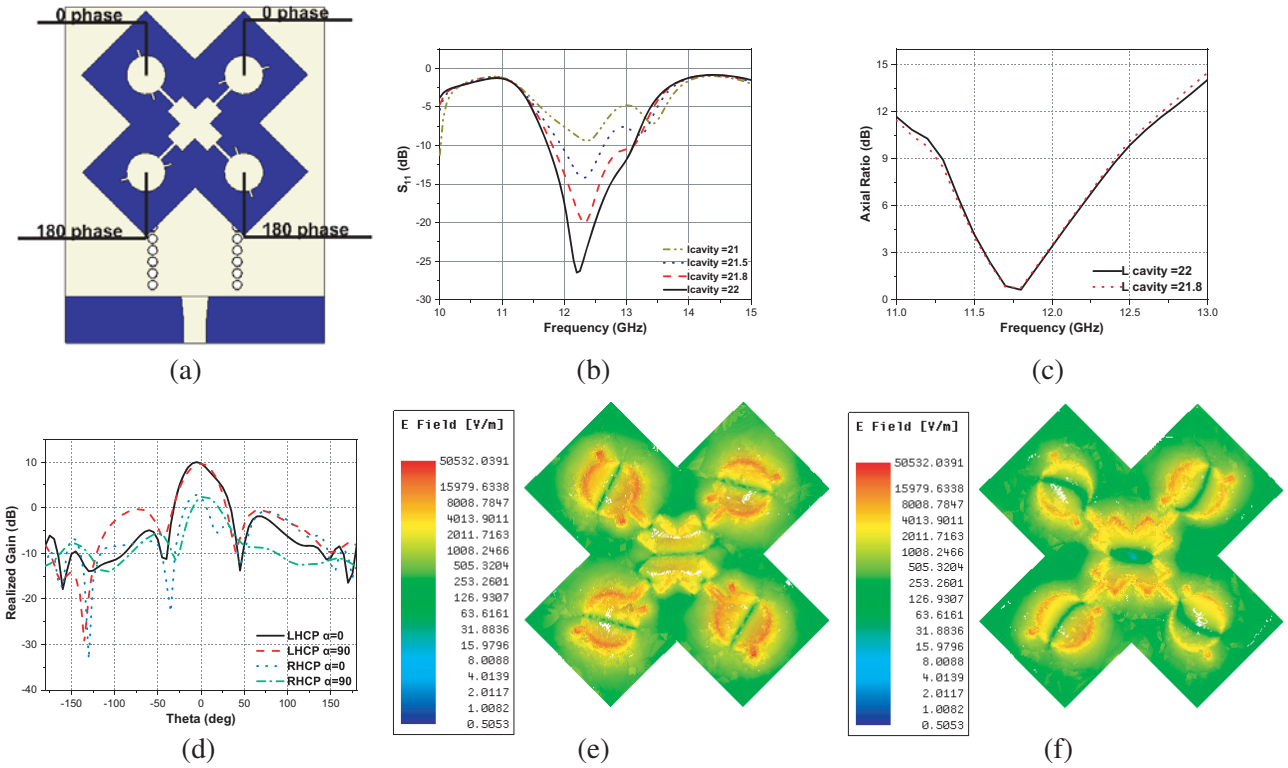

Figure 4. The initial design including. (a) The phase of each patch, (b) and (c) are RL and AR at various values of L_{cavity} in dB, (d) the LHCP and RHCP at the two planes [L_{cavity} = 22 mm at 12.3 GHz]. (e) and (f) the electric field at $\frac{1}{4}$ and $\frac{3}{4}$ of a period time (T), respectively.

Table 4. The optimized parameters of the [2 × 2] initial design.

parameter	description	Value
L_{stub}	Stub length	1.5 mm
W_{stub}	Stub width	0.44 mm
θ	Rotation angle	50°
a	Minor axis	8.662 mm
b	Major axis	8.662 mm
p	Distance between two via	2 mm
d	Vias diameter	1.75 mm
W_{slot}	The slot width	0.8 mm
L_{slot}	The slot length	13 mm
$D_{aperture}$	Distance between via and blocked via	10 mm
L_{cavity}	The cavity length	22 mm
$W_{opening}$	The width of the cavity open	10.8 mm
W_{taper}	The tapper input width	4.8 mm
W_{input}	The width of the input line	3.8 mm
W_{SIW}	The SIW width	15 mm
L_{SIW}	The SIW length	41 mm

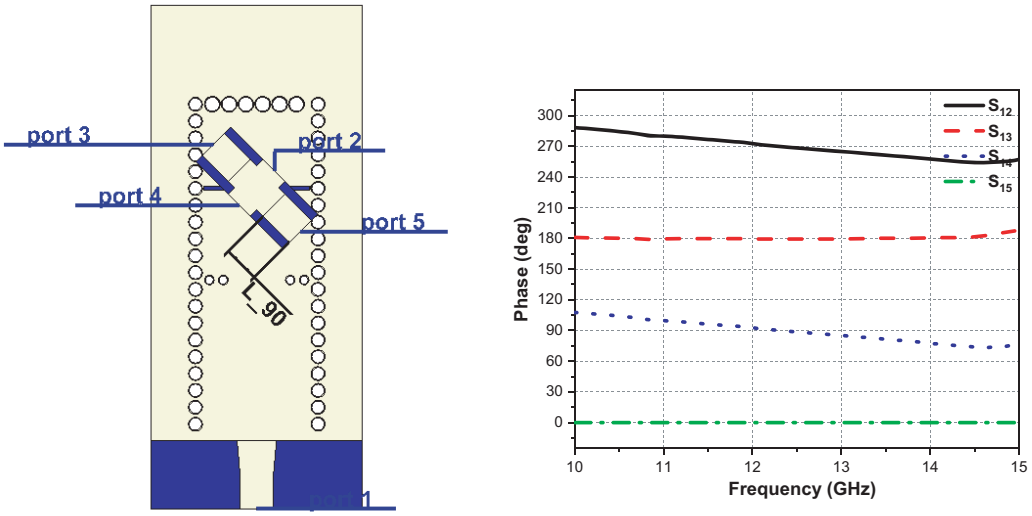

Figure 5. Front view of the sequential feeding network.

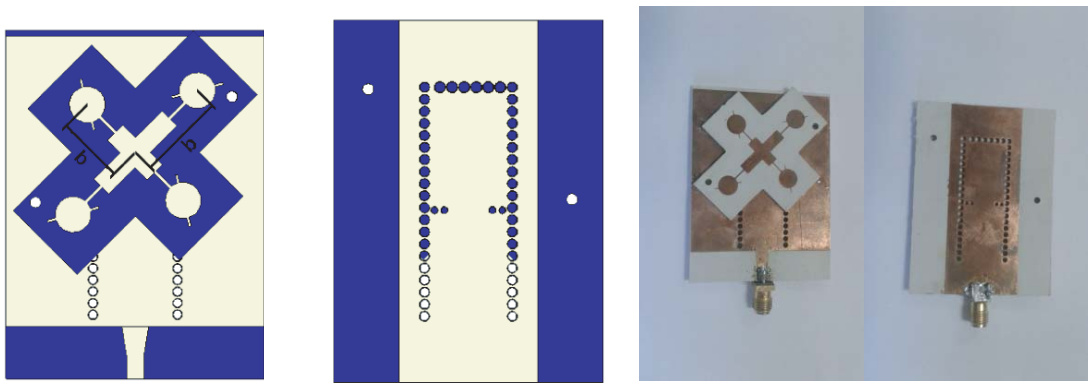

Figure 6. Sequential feeding elliptical array. The simulation (a) front view and (b) back view. The fabricated Sequential feeding elliptical array. (a) Front view and (b) back view.

Table 5. Optimized parameter for [2 × 2] elliptical array.

parameter	description	Value (mm)
W_{stub}	Stub width	0.4
W_{slot}	The slot width	0.58
L_{cavity}	The cavity length	21

5. [4 × 4] DOUBLE SEQUENTIAL FEEDING ELLIPTICAL ARRAY

Figure 7 illustrates simulation and measurement RLs, ARs, axial ratios beamwidths, electric field distributions, total gains, and the realized gains at 12.3 GHz. As mentioned previously, the cavity length, L_{cavity}, has a great effect on the RLBW and a slight effect on the ARBW as shown in Figs. 7(a) and (b). Selecting the cavity length to be $L_{cavity} = 21$ mm, a wide beamwidth (almost 65°) is achieved, as can be seen in Figure 7(c). Figs. 7(d), (e), and (f) present the fields that rotate in clockwise to

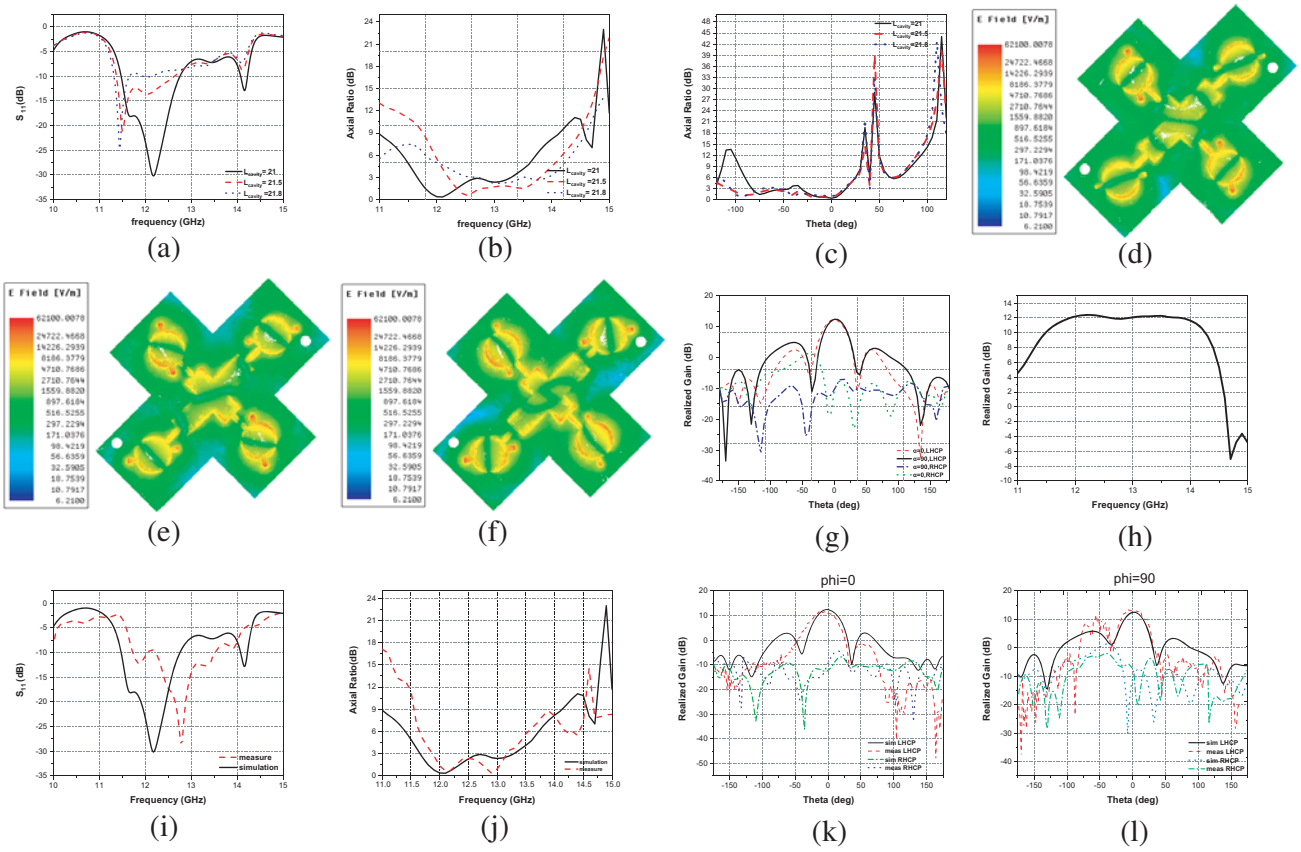

Figure 7. Simulation and measurement results of the $[2 \times 2]$ sequential feeding array. (a) and (b) are RL and AR at various values of L_{cavity} versus frequency, (c) the broadside pattern with the AR. (d), (e), and (f) are the electric field distributions in a period of time (T) at 12.3 GHz, $t = \frac{1}{4}, \frac{1}{2}, \frac{3}{4}$ T, respectively. (g) The broadside realized gain, (h) comparison between the measured and simulated RL, (i) the measured and simulated AR, (j) and (k) comparison between simulation and measured LHCP and RHCP at $\phi = 0°$ and 90°, respectively, at 12.3 GHz.

produce LHCP field, and consequently, a very good co-polarized to x-polarized ratio (> 15 dBi) in the main beam is achieved, as shown in Fig. 7(g). From Fig. 7(h), it can be seen that the gain is stable over the operating RLBW.

The measurement results show a good agreement with the simulation one. As can be seen from Fig. 7(i), the simulation and measurement RLBWs are from 11.47 to 12.76 GHz (10.75% BW) and from 11.73 to 13.52 GHz (15% BW), respectively. Furthermore, the measurement has a larger RLBW, but it is shifted about 200 MHz which, we believe, happens due to fabrication errors. The measured AR has almost 11.25% BW from 11.85 to 13.2 GHz while the simulation has around 13.6% BW from 11.66 to 13.29 GHz. Figs. 7(k) and (l) show a good agreement between the measurement and simulation field results. The figures illustrate that the gain is about 12 dBi, and the LHCP to the RHCP ratio is more than 15 dBi in the broadside direction.

To overcome the undesired radiation from the feed network and thus contributes to the polarization purity and radiation, as illustrated in [33], in addition to obtain high gain, a $[4 \times 4]$ double sequential feeding array is designed as presented in Fig. 8. The $[2 \times 2]$ elliptical array presented in Section 4 is used as a building block and sequentially fed with the same feeding network used to construct it (Fig. 5) to build the $[4 \times 4]$ array. The design dimensions are as illustrated in Table 4, except the final array size presented in Table 6.

Figure 9 presents the simulation result of a $[4 \times 4]$ double sequential feeding elliptical array. As

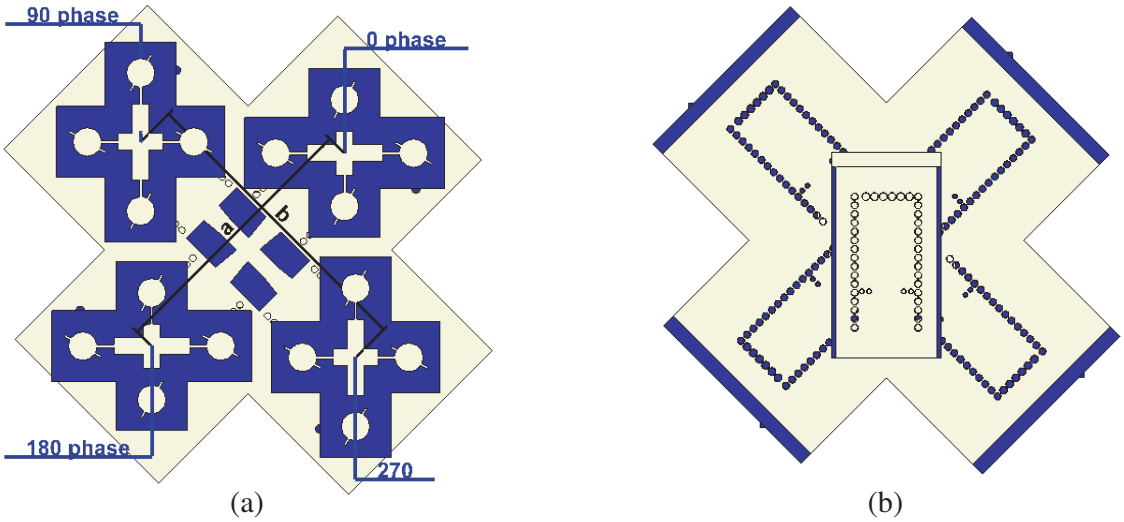

(a) (b)

Figure 8. Show the [4 × 4] array. (a) The front view and (b) back view of the design.

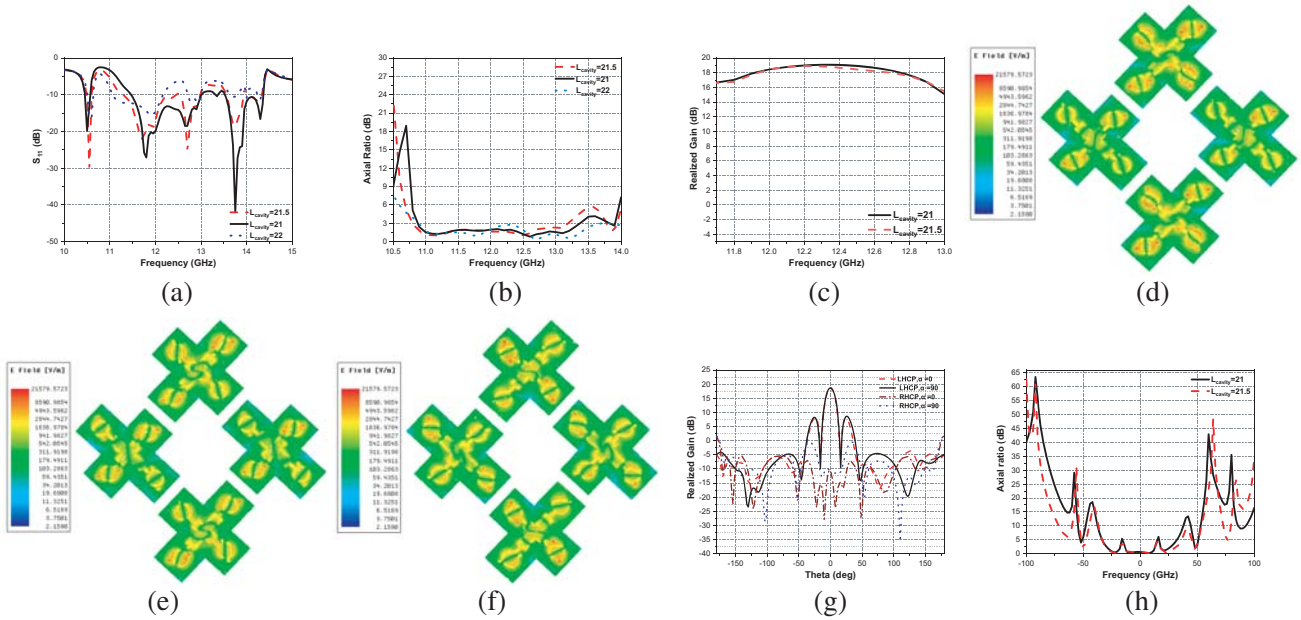

(a) (b) (c) (d) (e) (f) (g) (h)

Figure 9. A [4 × 4] elliptical array simulation. (a), (b), and (c) are RL, AR, and the realized gain at various values of L_{cavity}. (d), (e), and (f) are the electric field distributions in a period of time (T) at 12.3 GHz, at $t = 0, \frac{1}{4}, \frac{1}{2}$ T, respectively. (g) The realized gain in LHCP and RHCP in both plans at 12.3 GHz, (h) the beam pattern with AR.

Table 6. Final dimension of the [4 × 4] array.

parameter	description	Value (mm)
a	Minor axis	61.5
b	Major axis	65.6

noticed in the previous designs in Sections 4 and 3, L_{cavity} has a noticeable effect, as seen in Figs. 9(a) and (b) with $L_{cavity} = 21$ mm, and the broadest RLBW from 11.45 to 13 GHz (13% BW) and the broadest ARBW from 10.8 to 13.44 GHz (22% BW) are achieved. From Figs. 9(c) to (f) the propagation rotates in clockwise, and consequently, an LHCP field is propagated following the right-hand rule. Fig. 9(g) shows a very good LHCP to RHCP ratio more than 25 dBi. In addition to that, Fig. 9(h) shows a wide beam lower than 3-dB axial ratio about 20°.

6. RESULT AND DISCUSSION

All the simulations have been done by HFSS V18 and the measurement using Agilent N9918A vector network analyzer, and the connector that has been used in the fabrication is a gold-plated connector which supports our operating band, while the field measurements are done by Star Lab-18. The antenna arrays and feeding networks are fabricated using the same substrate (rogers 3003 with $\epsilon_r = 3$, substrate height $h = 1.525$, and tangent loss $\delta = 0.0013$). The substrate is appropriate to get a good quality factor in addition to its low cost. All the measured results have a very good agreement with the simulated one.

In Table 7, our design achieves higher gain than the reported CP antenna arrays with the same structure [4 × 4] and has wider ARBW than any other previously studied array. Furthermore, the proposed array is more than three-times in ARBW of the arrays in [2, 3], which work on the same band. Moreover, the proposed array could be easily manufactured and has a low profile.

Table 7. Design comparisons of the CP antenna arrays reported in the literature to date.

Ref.	No. of elements	Size ($\times\lambda_o$)	ARBW %	RLBW %	Realized gain	Complexity
[4]	2 × 2	2 × 3 × 0.18	6.7	6.6	12.5 dBic	moderate
[5]	4 × 4	3 × 3 × 0.39	10.7	6	15 dBic	complex
[6]	4 × 4	4 × 4 × 0.19	15.6	17.8	16 dBic	moderate
[34]	8 × 8	6.12 × 6.8 × 0.44	16.5	18.2	26.1 dBic	moderate
[7]	4 × 4	2.4 × 2 × 0.4	21.6	20	15 dBi	complex
[8]	4 × 4	2.8 × 3.2 × 0.22	19	27.5	16 dBi	moderate
[9]	16 × 16	29 × 29 × 1.12	12	10.5	30 dBi	moderate
[2]	16 × 6	13 × 5.3 × 0.05	6.16	8.2	26.4 dBic	easy
[3]	16 × 1	12 × 12 × 0.26	8.2	8.2	18.4 dBic	complex
Our work	4 × 4	4.2 × 4.2 × 0.18	22	13	19 dBi	easy

Table 8. Our work conclusion results.

Type	RLBW		ARBW		Gain		Size
	Sim(%)	Meas(%)	Sim(%)	Meas(%)	Sim(%)	Meas(%)	$\times\lambda_o$
Element	8.9	12	3	2.7	6.5	6.9	0.6 × 0.58 × 0.051
2×2 array	10.75	14.8	13.6	11.25	12.5	12	1.9 × 2.2 × 0.12
4×4 array	13	-	22	-	19	-	4.2 × 4.4 × 0.18

7. CONCLUSION

A wide axial ratio and return loss bandwidth, as well as low size, low profile and high gain circular polarized array is illustrated in this paper. Based on a study to meet the best requirements a novel circular microstrip patch is designed which has a good RLBW and ARBW. By choosing SIW as the feeding network and circular array as the antenna type, a new $[2 \times 2]$ circular array has been designed which gets good RLBW, however, low ARBW, so a novel compact sequential feeding network is designed to construct a $[2 \times 2]$ elliptical sequential feeding array which has a very good specification (RLBW, ARBW, size, profile, and gain). Extended work has been done to increase the obtained gain by designing a $[4 \times 4]$ double sequential feeding in which $[2 \times 2]$ has been used as the basic unit to build this array. Table 8 concludes the work, with a comparison between simulation and fabrication works, which show a good agreement between them. From this result, it has been found that this array is a good choice for wireless systems preferring high gain CP antennas with wide operating frequency, in particular, Ku-band satellite communication applications.

REFERENCES

1. Gao, S. S., Q. Luo, and F. Zhu, *Circularly Polarized Antennas*, John Wiley & Sons, 2013.
2. Huang, J., W. Lin, F. Qiu, C. Jiang, D. Lei, and Y. J. Guo, "A low profile, ultra-lightweight, high efficient circularly-polarized antenna array for ku band satellite applications," *IEEE Access*, Vol. 5, 18356–18365, 2017.
3. Alieldin, A., Y. Huang, M. Stanley, and S. Joseph, "A circularly polarized circular antenna array for satellite TV reception," *2018 15th European Radar Conference (EuRAD)*, 505–508, IEEE, 2018.
4. Guntupalli, A. B. and K. Wu, "60-GHz circularly polarized antenna array made in low-cost fabrication process," *IEEE Antennas and Wireless Propagation Letters*, Vol. 13, 864–867, 2014.
5. Li, Y., Z. N. Chen, X. Qing, Z. Zhang, J. Xu, and Z. Feng, "Axial ratio bandwidth enhancement of 60-GHz substrate integrated waveguide-fed circularly polarized LTCC antenna array," *IEEE Transactions on Antennas and Propagation*, Vol. 60, No. 10, 4619–4626, 2012.
6. Li, M. and K.-M. Luk, "Low-cost wideband microstrip antenna array for 60-GHz applications," *IEEE Transactions on Antennas and Propagation*, Vol. 62, No. 6, 3012–3018, 2014.
7. Liu, C., Y.-X. Guo, X. Bao, and S.-Q. Xiao, "60-GHz LTCC integrated circularly polarized helical antenna array," *IEEE Transactions on Antennas and Propagation*, Vol. 60, No. 3, 1329–1335, 2011.
8. Sun, H., Y.-X. Guo, and Z. Wang, "60-GHz circularly polarized U-slot patch antenna array on LTCC," *IEEE Transactions on Antennas and Propagation*, Vol. 61, No. 1, 430–435, 2012.
9. So, K. K. and C. H. Chan, "Circularly polarized patch antenna array for satellite communication in ku band," *2016 10th European Conference on Antennas and Propagation (EuCAP)*, 1–4, IEEE, 2016.
10. Ioannides, P. and C. A. Balanis, "Uniform circular and rectangular arrays for adaptive beamforming applications," *IEEE Antennas and Wireless Propagation Letters*, Vol. 4, 351–354, 2005.
11. Chang, F.-S., K.-L. Wong, and T.-W. Chiou, "Low-cost broadband circularly polarized patch antenna," *IEEE Transactions on Antennas and Propagation*, Vol. 51, No. 10, 3006–3009, 2003.
12. Esselle, K. P., A. Verma, et al., "Wideband circularly polarized stacked microstrip antennas," *IEEE Antennas and Wireless Propagation Letters*, Vol. 6, 21–24, 2007.
13. Guo, Y.-X. and D. C. H. Tan, "Wideband single-feed circularly polarized patch antenna with conical radiation pattern," *IEEE Antennas and Wireless Propagation Letters*, Vol. 8, 924–926, 2009.
14. Lin, C., F.-S. Zhang, Y.-C. Jiao, F. Zhang, and X. Xue, "A three-fed microstrip antenna for wideband circular polarization," *IEEE Antennas and Wireless Propagation Letters*, Vol. 9, 359–362, 2010.
15. Qing, X., "Broadband aperture-coupled circularly polarized microstrip antenna fed by a three-stub hybrid coupler," *Microwave and Optical Technology Letters*, Vol. 40, No. 1, 38–41, 2004.
16. Kilgus, C., "Shaped-conical radiation pattern performance of the backfire quadrifilar helix," *IEEE Transactions on Antennas and Propagation*, Vol. 23, No. 3, 392–397, 1975.

17. Chen, Y.-Y. and K.-L. Wong, "Low-profile broadband printed quadrifilar helical antenna for broadcasting satellite application," *Microwave and Optical Technology Letters*, Vol. 36, No. 2, 134–136, 2003.
18. Keen, K., "Bandwidth dependence of resonant quadrifilar helix antennas," *Electronics Letters*, Vol. 46, No. 8, 550–552, 2010.
19. Pan, Y. and K. W. Leung, "Wideband circularly polarized trapezoidal dielectric resonator antenna," *IEEE Antennas and Wireless Propagation Letters*, Vol. 9, 588–591, 2010.
20. Deng, S.-M. and C.-L. Tsai, "A broadband slot-coupled circularly polarized rectangular notch dielectric resonator antenna fed by a microstrip line," *2005 IEEE Antennas and Propagation Society International Symposium*, Vol. 4, 246–249, IEEE, 2005.
21. Pan, Y. and K. W. Leung, "Wideband omnidirectional circularly polarized dielectric resonator antenna with parasitic strips," *IEEE Transactions on Antennas and Propagation*, Vol. 60, No. 6, 2992–2997, 2012.
22. Khalily, M., M. K. Rahim, and A. A. Kishk, "Planar wideband circularly polarized antenna design with rectangular ring dielectric resonator and parasitic printed loops," *IEEE Antennas and Wireless Propagation Letters*, Vol. 11, 905–908, 2012.
23. Wong, K.-L., J.-Y. Wu, and C.-K. Wu, "A circularly polarized patch-loaded square-slot antenna," *Microwave and Optical Technology Letters*, Vol. 23, No. 6, 363–365, 1999.
24. Row, J.-S. and S.-W. Wu, "Circularly-polarized wide slot antenna loaded with a parasitic patch," *IEEE Transactions on Antennas and Propagation*, Vol. 56, No. 9, 2826–2832, 2008.
25. Han, T.-Y., Y.-Y. Chu, L.-Y. Tseng, and J.-S. Row, "Unidirectional circularly-polarized slot antennas with broadband operation," *IEEE Transactions on Antennas and Propagation*, Vol. 56, No. 6, 1777–1780, 2008.
26. Hwang, K., "Broadband circularly-polarised spidron fractal slot antenna," *Electronics Letters*, Vol. 45, No. 1, 3–4, 2009.
27. Cohn, S. B., "Characteristic impedance of the shielded-strip transmission line," *Transactions of the IRE Professional Group on Microwave Theory and Techniques*, Vol. 2, No. 2, 52–57, 1954.
28. Simons, R. N., *Coplanar Waveguide Circuits, Components, and Systems*, Vol. 165. John Wiley & Sons, 2004.
29. Nawaz, M. I., Z. Huiling, and M. Kashif, "Substrate Integrated Waveguide (SIW) to microstrip transition at X-band," *Proceedings of the 2014 International Conference on Circuits, Systems and Control*, 61–63, 2014.
30. Xu, F. and K. Wu, "Guided-wave and leakage characteristics of substrate integrated waveguide," *IEEE Transactions on Microwave Theory and Techniques*, Vol. 53, No. 1, 66–73, 2005.
31. Balanis, C. A., *Antenna Theory: Analysis and Design*, John Wiley & Sons, 2016.
32. Hall, P., "Application of sequential feeding to wide bandwidth, circularly polarised microstrip patch arrays," *IEE Proceedings H (Microwaves, Antennas and Propagation)*, Vol. 136, 390–398, IET, 1989.
33. Chen, A., Y. Zhang, Z. Chen, and C. Yang, "Development of a ka-band wideband circularly polarized 64-element microstrip antenna array with double application of the sequential rotation feeding technique," *IEEE Antennas and Wireless Propagation Letters*, Vol. 10, 1270–1273, 2011.
34. Li, Y. and K.-M. Luk, "A 60-GHz wideband circularly polarized aperture-coupled magneto-electric dipole antenna array," *IEEE Transactions on Antennas and Propagation*, Vol. 64, No. 4, 1325–1333, 2016.